Materials Advances

ROYAL SOCIETY OF CHEMISTRY

PAPER

View Article Online
View Journal | View Issue

Cite this: *Mater. Adv.*, 2024, 5, 7446

Synthesis of a thermoplastic elastomer from α-methylene-γ-butyrolactone for high temperature applications†

Friso G. Versteeg, [a] Théophile Pelras, [b] Giuseppe Portale [c] and Francesco Picchioni *[a]

Thermoplastic elastomers, such as polystyrene-*b*-polybutadiene-*b*-polystyrene (SBS), are essential components in a wide array of industries, from seals and gaskets in building construction to binders in Li-ion batteries. However, SBS rubbers are still produced from 100% oil-based materials and their use is limited by relatively low thermal stability. When used in applications where temperatures exceed 100 °C, their mechanical properties become poor and at temperatures above 140 °C a cross-linking reaction is typically triggered. This factually cures (*i.e.* crosslinks) the system, hardening the rubber and hindering recycling, which is a prominent limitation of SBS rubbers. α-Methylene-γ-butyrolactone (MBL) is a monomer that has recently been under the spotlight, thanks to its bio-renewable nature and the high thermal stability of its corresponding polymer. While a promising candidate for the next generation of thermoplastic elastomers, its successful implementation in functional products has yet to be demonstrated. Herein, we report a simple methodology to produce high quantities of SBS-like elastomers based on BAB terblock copolymers featuring a MBL segment and hexyl methacrylate (HMA) segment, poly(MBL)-*block*-poly(HMA)-*block*-poly(MBL). A two-step reversible addition–fragmentation chain-transfer polymerisation using a bis-functional chain-transfer agent ensured controlled and symmetrical growth of the blocks. Tailoring the monomer ratio in the chain-extension step enables the production of copolymers with varying hard/soft block ratios, allowing for tuning of the mechanical properties of the elastomers. Their high thermal stability and the absence of temperature-induced cross-links further enable the remoulding of the rubber without any losses of mechanical properties.

Received 5th June 2024,
Accepted 26th August 2024

DOI: 10.1039/d4ma00583j

rsc.li/materials-advances

1. Introduction

Thermoplastic elastomers (TPEs) are biphasic materials in their temperature range of utilization and typically consist of linear ABA terblock copolymers featuring soft inner blocks and hard outer segments.[1] The most commonly used TPE worldwide, polystyrene-*b*-polybutadiene-*b*-polystyrene (SBS), comprises one rubbery polybutadiene (PB) segment covalently linked to two rigid polystyrene (PS) chains. This structure grants excellent properties within its temperature range of applications, which is between the glass transition temperatures of its two components ($T_{g\,PB}$ = −40 °C and $T_{g\,PS}$ = 100 °C).[2,3] However, not only is this TPE completely produced from oil-based materials, but it also possesses limited applicability at temperatures above 100 °C, where its mechanical properties drastically decrease. Thus, the key to the successful implementation of elastomers in high-temperature applications lies in the increase of their T_g.

Multiple studies have attempted to blend SBS with other polymers exhibiting a higher T_g than polystyrene, *e.g.* (poly(2,6-dimethyl-1,4-phenylene oxide)).[4–7] However, drastic improvements were not observed, supposedly due to the absence of chemical interactions between the components. Another potential candidate for blending is poly(α-methylene-γ-butyrolactone) (PMBL), which not only features a high glass transition temperature (T_g ∼ 195 °C), but also good chemical resistance. In addition, it is a monomer derived from biomass.[8–11] In a previous study, SBS was blended with a PS-*b*-PMBL block copolymer to not only enhance its mechanical properties, but also to limit de-mixing of the two chains.[12] While the blends

[a] *Department of Chemical Engineering – Product Technology, University of Groningen, Nijenborgh 4, 9747 AG Groningen, The Netherlands. E-mail: f.picchioni@rug.nl*
[b] *Macromolecular Chemistry and New Polymeric Materials, Zernike Institute for Advanced Materials, University of Groningen, Nijenborgh 4, 9747 AG, The Netherlands*
[c] *Physical Chemistry of Polymeric and Nanostructured Materials, Zernike Institute for Advanced Materials, University of Groningen, 9747 AG Groningen, The Netherlands*

† Electronic supplementary information (ESI) available. See DOI: https://doi.org/10.1039/d4ma00583j

indeed showed improved mechanical properties, internal crosslinking of the polybutadiene occurred at the required high working temperatures, which decreased the elasticity of the blends. Furthermore, due to the crosslinked network, the recyclability becomes arduous and the breaking of the crosslinked bonds damages the polymer structure as well.[13]

Crosslinking between the unsaturated double bond of polybutadiene (*i.e.* through exposure to UV, oxidation or temperature) is yet another hurdle in the design of thermally-stable TPEs.[14,15] To remedy this, the synthesis of star-like poly(*n*-butyl acrylate)-*b*-poly(α-methylene-γ-butyrolactone) block copolymers *via* atom transfer radical polymerisation (ATRP) has been investigated.[16] While the poly(*n*-butyl acrylate) block did feature a low T_g without being subject to thermal crosslinking, a major disadvantage of ATRP is that the copper catalyst must be removed from the product, rendering the process more difficult to implement at a larger, commercially feasible scale due to the high costs of purification.[17,18]

Herein, we report the two-step synthesis of linear BAB terblock copolymers comprising a soft/rubbery poly(*n*-hexyl methacrylate) (PHMA) inner block and two hard PMBL outer segments using metal catalyst-free reversible addition–fragmentation chain-transfer (RAFT) polymerisation (Scheme 1). The use of a bis-functional chain-transfer agent enables good control of the chain lengths and growth of a symmetric BAB polymer. In the ESI,† the RAFT mechanism is discussed in more detail in Fig. S1.[19] By simply varying the α-MBL concentration during the second polymerisation step, it is possible to obtain polymers with different PMBL chain lengths (*i.e.* varying soft/hard block ratio), which directly influences the mechanical properties of the thermoplastic elastomers.

2. Materials and methods

2.1. Chemicals

Ethylene glycol (EG, ≥99.8%, anhydrous, CAS 107-21-1) and dichloromethane (DCM, 99.8%, anhydrous, CAS 75-09-2) were sourced from Acros Organics. Magnesium sulphate ($MgSO_4$, dried, extra pure, CAS 7487-88-9) and sodium chloride (NaCl, technical grade, CAS 7647-14-5) were acquired from Boom. Ethyl acetate (AR grade, CAS 141-78-6) and *n*-hexane (AR grade, CAS 110-54-3) were obtained from Macron Fine Chemicals. Absolute ethanol (99.9%, CAS 64-17-5) was purchased from J. T. Baker. Acetone (AR grade, CAS 67-64-1), methanol (AR grade, CAS 67-56-1), aluminium oxide (AlOx, basic activated, CAS 1344-28-1), 2,2′-azobis(2-methylpropionitrile) (AIBN, 98%, CAS 78-67-1), 4-cyano-4-(phenylcarbonothioylthio)pentanoic acid (CTBPA, CAS 201611-92-9), *N*-(3-dimethylaminopropyl)-*N*′-ethylcarbodiimide hydrochloride (EDC·HCl, for synthesis, CAS 1892-57-5), 4-dimethylaminopyridine (DMAP, ≥99%, CAS 1122-58-3), *N*,*N*-dimethylformamide (DMF, 99+ anhydrous, CAS 68-12-2), methyl methacrylate (MMA, 99%, CAS 80-62-6), hexyl methacrylate (HMA, 99%, CAS 142-09-6) and sodium bicarbonate ($NaHCO_3$, ≥99.7%, CAS 144-55-8) were purchased from Sigma-Aldrich. Silica gel P60 (40–63 μm) was sourced from silicycle. Hexyl methacrylate and methyl methacrylate were purified by glass chromatography using silica before use to remove any inhibitor. α-Methylene-γ-butyrolactone (α-MBL, >95% purity, CAS 547-65-9) was purchased from TCI. Chemicals were used as received without further purification, with the exception of AIBN that was purified by recrystallization in methanol twice.

2.2. Preparation of the bis-functional RAFT agent

The synthesis was performed according to previously reported protocols, with adaptations.[20,21] CTBPA (989 mg, 3.55 mmol), EG (96.0 mg, 1.55 mmol) and 15 mL dry DCM were added to a round bottom flask equipped with a stirring egg, cooled over an ice bath and sparged with argon. In a separate glass vial, EDC·HCl (932 mg, 4.86 mmol) and DMAP (46.8 mg, 0.384 mmol) were dispersed in 15 mL dry DCM and added dropwise into the reaction mixture under argon flow. The vessel was allowed to slowly warm up to room temperature and left to stir for 18 h. Then, the reaction mixture was further diluted with 20 mL DCM and washed twice with 150 mL 0.1 M $NaHCO_3$ and once with 150 mL 0.1 M NaCl, before drying with $MgSO_4$ *in vacuo*. The bis-functional RAFT agent was purified through flash column chromatography using a 3 : 2 *n*-hexane : ethyl acetate mixture as eluent ($R_f \approx 0.3$). Only the purest fractions were kept and

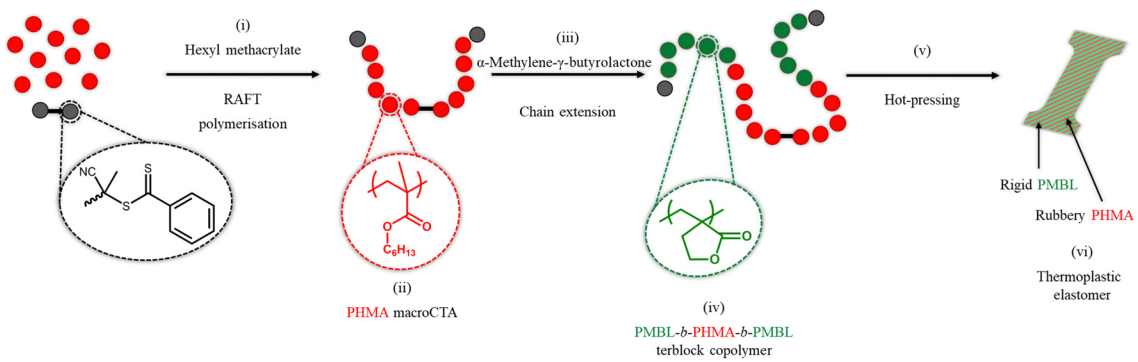

Scheme 1 Synthesis of a linear terblock copolymer and its use as a thermoplastic elastomer.[a] [a] (i) RAFT polymerisation of hexyl methacrylate is performed using a bis-functional chain transfer agent to produce (ii) a PHMA macroCTA, followed by (iii) chain extension with α-methylene-γ-butyrolactone to yield (iv) a rigid/soft PMBL-*b*-PHMA-*b*-PMBL terblock copolymer. (v) The polymer is moulded into a dog-bone shape through hot-pressing to create a recyclable thermoplastic elastomer.

concentrated *in vacuo* to yield a viscous dark pink/red liquid with a final yield of 467 mg (45%).

Note that a larger batch was produced using 8.0 g CTBPA, 796 mg EG, 6,80 g EDC·HCl and 371 mg DMAP and provided 3.42 g of purified bisCTBPA (yield = 20%). The lower yield originates from large losses during flash column chromatography (*i.e.* interactions with the stationary phase) and the combination of only the purest fractions collected.

2.3. Preparation of poly(hexyl methacrylate) (PHMA) macroCTA

A typical polymerisation was conducted as follows: hexyl methacrylate (25 g, 0.146 mol), bisCTBPA (0.25 g, 0.428 mmol), AIBN (0.01 g, 0.06 mmol) and DMF (150 mL) were added to a 250 mL round bottom flask equipped with a magnetic stirrer. Once all the compounds were added, the flask was sealed with a rubber septum and paraffin wax and flushed with argon for 45 minutes. The mixture was then heated up in an oil bath at 80 °C and stirred at 350 rpm to initiate the RAFT polymerisation. The total reaction time was set to be 24 hours. The product, PHMA, was obtained by precipitating the mixture in ice-cold methanol at a volumetric ratio of 1 : 10 of DMF to methanol. This wash was repeated three times to remove all excess monomer and DMF. Subsequently, the product was transferred to a 250 mL round bottom flask and dried overnight in a vacuum oven at 65 °C. The molecular weight (M_n) and dispersity index ($Đ$) were determined using GPC with a yield of 13.0 g (52%) on average.

2.4. Synthesis of PMBL-*b*-PHMA-*b*-PMBL

The preparation of the terblock copolymer follows the same protocol described in Section 2.3. However, the formed PHMA polymer will act as a macroCTA. A typical synthesis is according to the following procedure: PHMA (13.0 g 0.39 mmol), AIBN (9.2 mg, 0.05 mmol), α-MBL (15 g, 0.15 mol) and DMF (150 mL) were added to a 250 mL round bottom flask equipped with a magnetic stirrer. The flask was then sealed with a rubber septum and paraffin wax and flushed with argon for 45 minutes. The mixture was then placed in an oil bath set to 80 °C and 350 rpm and left to react for 24 hours. After the reaction, the terblock copolymer product was precipitated in ice-cold methanol at a volumetric ratio of 1 : 5 of DMF to methanol and filtered using a Buchner funnel. Finally, the terblock copolymer was dried overnight in a vacuum oven at 125 °C. The molecular weight (M_n) and dispersity index ($Đ$) were determined using GPC with a yield of 22 g (78.5%) on average.

2.5. Gel permeation chromatography (GPC)

GPC analyses were performed using a Hewlett Packard 1100 series with 3× Agilent Technologies PL gel Mixed E analytical linear columns (300 × 7.5 mm 3 μm) at a flowrate of 1 mL min^{-1} at 40 °C with an injection volume of 20 μL. The eluent of the system was THF and M_n, M_w and $Đ$ were determined from refractive index chromatograms using polystyrene standards by using an Agilent 1200 refractive index detector with toluene as the reference peak. The terblock copolymer GPC analysis was performed using an Agilent model 1200 series with 3× PSS GRAM analytical linear columns (300 × 8 mm 10 μm) at a flowrate of 1 mL min^{-1} at 50 °C with an injection volume of 20 μL. The eluent of the system was DMF with 10 mM LiBr and M_n, M_w and PDI were determined from refractive index chromatograms using polystyrene standards by using an Agilent 1200 refractive index detector with toluene as the reference peak.

2.6. Fourier-transform infrared spectroscopy (FTIR)

FTIR measurements were performed in order to characterize the PMBL samples. Each sample was measured from 600–4000 cm^{-1}, using a resolution of 4 cm^{-1}, 2–4 times.

2.7. Thermogravimetric analyses

The decomposition temperature of the products was determined by thermogravimetric analysis on a TA TGA 550. Under nitrogen atmosphere or air, samples were heated from 25 °C to 600 °C at 20 °C min^{-1}. Data were processed using TA instruments software.

2.8. Differential scanning calorimetry

DSC analysis of polymer samples was performed on a TA instruments Discovery DSC 25 equipped with a cooler and auto sampler. Samples were prepared in a Tzero aluminium pan and were analysed in the following method: −20 °C to 220 °C at 10 °C min^{-1} heating rate, 220 °C to 100 °C at 10 °C min^{-1} cooling rate and finally −20 °C to 220 °C at 10 °C min^{-1} heating rate. The T_g of the polymers was detected in the second heating rate and processed by the software Trios.

2.9. Nuclear magnetic resonance (NMR) spectroscopy

^{1}H- and ^{13}C-NMR analyses were performed on either an Oxford NMR AS 400 or an Oxford NMR AS 500 spectrometer operating at 400 and 500 MHz, respectively. The bis-functional RAFT agent and homopolymer were measured at 25 °C and 400 MHz in deuterated chloroform ($CDCl_3$, 99.9%, Sigma-Aldrich) while the terblock copolymers were measured at 75 °C and 500 MHz in deuterated DMF.

2.10. Small angle X-ray scattering (SAXS)

Small angle X-ray scattering (SAXS) measurements were performed using a multipurpose X-ray device for nanostructured analysis (MINA) instrument at the University of Groningen. The instrument is built around a Cu rotating anode X-ray source, delivering a high flux beam with a wavelength of 0.15413 nm (E = 8 keV). The SAXS data have been acquired using a 2D Pilatus 300 K Si solid state detectors (Dectris) placed 3.1 m away from the sample. The sample-to-detector distance and the beam centre were calibrated using the diffraction rings from a standard silver behenate powder. The samples were measured in the form of 1 mm thick compression moulded sheets. 10 min of exposure time was used. The 2D patterns were radially averaged around the beam centre to generate the 1D SAXS profiles of $I(q)$ *vs.* q, where q is the modulus of the scattering vector ($q = 4\pi \sin\theta/\lambda$ with 2θ being the scattering angle). After correction for sample absorption, the background of the empty

chamber was subtracted, being almost negligible concerning the scattering single of the block copolymers.

2.11. Shear rheometer

A Discovery Hybrid Rheometer DHR-2 from TA Instruments, equipped with a force rebalance transducer (FRT), was used for the rheological experiments. 8 mm diameter stainless steel parallel plates were used for all the experiments. The temperature was controlled *via* a convection oven fed with nitrogen gas to minimize sample degradation. Samples were shaped into disks using a hot-press at a temperature around the glass transition temperature of the sample and then cooled to room temperature. The following rheological protocol was adopted for the measurements: (i) dynamic strain amplitude sweep at ω = 100 rad s^{-1} to detect the linear viscoelastic regime, (ii) dynamic frequency sweep at strain amplitudes in the range of 1–5% and a frequency range between 100 and 0.1 rad s^{-1}. When switching temperature, a dynamic time sweep in the linear regime was performed in order to ensure stationary conditions, before performing (i) and (ii).

2.12. Tensile tests

Mechanical properties of the rubber blends were measured using a Tinius Olsen H2SKT set with a pulling speed of 10 mm min^{-1}. Samples were prepared by hot pressing the blends in dog-bone moulds with a thickness of approximately 1, gauge width of 5 mm and gauge length of approximately 22 mm, Fig. S13 (ESI†).

3. Results and discussion

3.1. Synthesis of the chain-transfer agent

First, a bis-functional chain-transfer agent (bisCTA) was produced to ensure the synthesis of truly symmetrical terblock copolymers. The compatibility between the CTA and the monomers was taken into consideration in the design strategy, thus a commercially-available cyano-methyl-dithiobenzoate was selected, as it is effective for the polymerisation of methacrylates and α-methylene-γ-butyrolactone (α-MBL).[8] A Steglich esterification between the acid group of 4-cyano-4-(phenylcarbonothioylthio)-pentanoic acid (CTBPA, 3.55 mol) and a small diol linker (ethylene glycol, 1.55 mole) was performed, following previously reported procedures with adaptations.[20,21] After purification with flash column chromatography and the collection of only the purest fractions, bisCTA was obtained in moderate yield (45 mol%, 0.47 g from 1.0 g CTA). Proton and carbon nuclear magnetic resonance spectroscopy (^{1}H NMR and ^{13}C NMR, Fig. S2 and S3, respectively, ESI†) confirmed the linkage of two CTA moieties (4H, δ 7.39 ppm; 2H, δ 7.56 ppm and 4H, δ 7.90 ppm) *via* the ethylene glycol bridge (4H, δ 4.34 ppm) and the high purity of the resulting bisCTA.

Before the formation of the terblock copolymers, a test polymerisation with methyl methacrylate (MMA) was conducted using our bisCTA (see ESI†). ^{1}H-NMR analyses on the resulting poly(methyl methacrylate) (PMMA) homopolymer evidenced a relatively high conversion (79%, DP_{PMMA} = 80, $M_{n\,NMR}$ = 8600 Da) and the presence of the benzoate end-groups, while gel permeation chromatography (GPC, Fig. S4, ESI†), confirmed a controlled polymerisation with low dispersity ($Đ_{PMMA}$ = 1.16) and the absence of chain–chain termination.

3.2. Synthesis of the bisfunctional macroRAFT agent of CTBPA-HMA-CTBPA

After synthesis of the bis-functional RAFT agent, an assortment of BAB terblock copolymers were produced, starting with a poly(hexyl methacrylate) middle segment. PHMA was chosen, as its low glass transition temperature (T_g = −5 °C) provides rubbery properties to the thermoplastic elastomer.[22] A series of PHMA homopolymers were produced using bisCTA, with AIBN as the initiator (typical [AIBN]:[RAFT] ratio of [1]:[7] to maintain good control over the reaction) and DMF as solvent, aiming at molecular weights of 30 kDa. With eqn (1) it is possible to predetermine the molecular weight of the PHMA segment by estimating a 50% conversion (X) for this polymerisation.

$$M_{n_{th}} = \frac{[M]_0}{[RAFT]_0} \times X \times MW_{monomer} + MW_{RAFT} \quad (1)$$

After purification, the chemical composition of the polymers was determined by ^{1}H-NMR (Fig. 1 and Fig. S7, ESI†). All polymerisations were conducted with adequate control, evidenced using GPC (Fig. 1 and Fig. S5, ESI†), showing narrow dispersities ($Đ \leq 1.3$) and relative similar theoretical and experimental molecular weights (Table 1).

3.3. Synthesis of poly(MBL-*b*-HMA-*b*-MBL)

Next, a series of poly(α-methylene-γ-butyrolactone)-*block*-poly(hexyl methacrylate)-*block*-poly(α-methylene-γ-butyrolactone) P(MBL-*b*-PHMA$_x$-*b*-PMBL)$_x$ terblock copolymers were synthesized using the PHMA macroCTAs and α-methylene-γ-butyrolactone. ^{1}H-NMR analyses on the purified polymers confirmed the

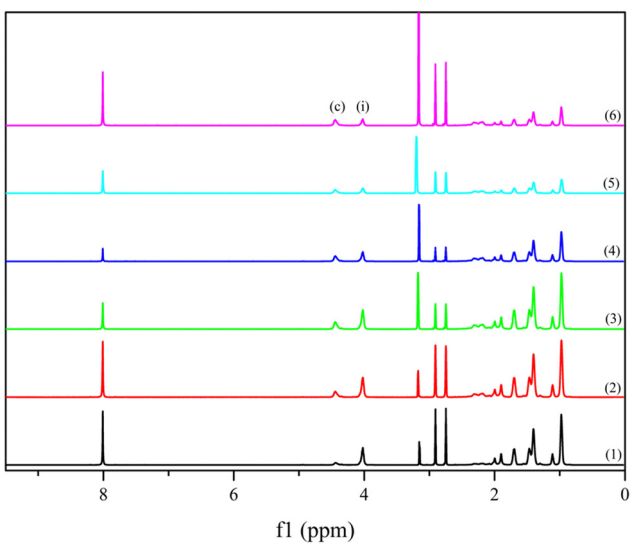

Fig. 1 ^{1}H NMR spectra of terblock copolymers; 1 denoting P(MBL-*b*-HMA$_1$-*b*-MBL)$_1$ and 6 P(MBL-*b*-HMA$_6$-*b*-MBL)$_6$.

Table 1 Results of the RAFT polymerisation of HMA at 80 °C, 24 hours and 350 rpm

Sample	M_n[a] (kDa)	$M_{n_{th}}$ (kDa)	Conv.[b] (%)	$Đ$[a]
$PHMA_1$	34	30	52	1.15
$PHMA_2$	35	30	58	1.14
$PHMA_3$	33	32	53	1.13
$PHMA_4$	25	32	45	1.32
$PHMA_5$	38	32	61	1.15
$PHMA_6$	32	32	55	1.16

[a] Determined by GPC in THF with 0.1 M toluene and calibrated against near-monodisperse PS standards. [b] Conversion determined gravimetrically after purification.

presence of α-MBL units in the structure (Fig. 1 and Fig. S8, ESI†) as well as the CTA end group that is still present in the terblock copolymer (Fig. S8, ESI†). In addition, it enabled calculation of the block ratio by comparison of the PMBL signals (i) (2H per MBL, δ 4.4 ppm) to the PHMA ones (c) (2H per HMA, δ 4.0 ppm). Additionally, GPC (Table 1 and Fig. S6, ESI†) showed proper chain extension, evidenced by a shift of the polymer signal and preservation of relatively narrow dispersities ($Đ < 1.4$, see Table 2). Finally, FTIR spectra confirmed the addition of MBL as the peak at 1644 cm^{-1} disappeared when comparing the terblock copolymer with pure MBL (Fig. S9, ESI†).[11] By simply varying the starting concentration of α-MBL monomer, different PMBL chain lengths and PHMA/PMBL block ratios were obtained, resulting in a series of P(MBL-*b*-HMA_x-*b*-MBL)$_x$ terblock copolymers with different ratios of outer hard/inner soft blocks (Fig. 1).

The thermal properties of the novel terblock-copolymers were determined, starting with thermogravimetric analyses (TGA, Fig. S11, ESI†). Both the reference homopolymer as well as the copolymers demonstrated a high thermal stability, up to ~250 °C, with onsets of degradation temperatures ranging between 320–338 °C. PHMA and PMBL homopolymers possess glass transition temperatures of $T_{g\,PHMA} = -5$ °C and $T_{g\,PMBL} =$ 195 °C, as evidenced by differential scanning calorimetry (DSC, Fig. S10, ESI†).[8,22] It must be noted that PMBL exhibits a T_g of 160 °C when the degree of polymerisation is below 50, or in other words, a chain length below 5 kDa.[23] Measurements performed on the terblock copolymers evidenced the presence of two distinctive glass transition temperatures, corresponding to that of PHMA and PMBL homopolymers and indicative of demixing of the blocks. It should be noted that a copolymer with short PMBL segments (*e.g.* P(MBL-*b*-$PHMA_1$-*b*-PMBL)$_1$) does not exhibit a T_g at high temperature, at least within the DSC detection range. Pelras *et al.* also observed a low T_g signal of one of the segments in the block copolymer when the molar fraction decreases.[24,25] Thus, TGA confirms that production of objects through hot-pressing is possible without damaging the structure of the polymers in an operating window above the T_g of PMBL but below the decomposition temperature of the terblock copolymer.

Table 2 Results of the RAFT block copolymerisation of MBL at 80 °C, 24 hours and 350 rpm

Sample	M_n[a] (kDa)	M_n[b] (kDa)	$M_{n_{th}}$ (kDa)	Conv.[c] (%)	$Đ$[a]
P(MBL-*b*-HMA_1-*b*-MBL)$_1$	40	41	40	72	1.34
P(MBL-*b*-HMA_2-*b*-MBL)$_2$	48	49	48	74	1.24
P(MBL-*b*-HMA_3-*b*-MBL)$_3$	54	51	52	77	1.41
P(MBL-*b*-HMA_4-*b*-MBL)$_4$	50	45	41	75	1.46
P(MBL-*b*-HMA_5-*b*-MBL)$_5$	61	68	62	78	1.54
P(MBL-*b*-HMA_6-*b*-MBL)$_6$	74	72	72	79	1.30

[a] Determined by GPC in DMF with 0.1 M toluene and calibrated against near-monodisperse PS standards. [b] Determined by ^{1}H-NMR using M_w from macroCTA. [c] Conversion determined gravimetrically after purification.

3.4. Morphological investigation

The phase separation behaviour and morphology of the terblock copolymers was investigated by SAXS. The 1D SAXS results for the P(MBL-*b*-$PHMA_1$-*b*-PMBL)$_1$ to P(MBL-*b*-$PHMA_6$-*b*-PMBL)$_6$ are summarized in Fig. 2. All investigated block copolymers (BCPs) show clear phase separated structure, indicating high chemical incompatibility between the two blocks. The main peak position revealed in SAXS provides the average spacing between adjacent domains of the same nature by the relationship $d_{AB} = \frac{2\pi}{q*}$, *i.e.* average interblock phase separation provided by the sum of the thickness of blocks A and block B. As expected, the average interblock spacing increases with increasing the overall BCP molecular weight. The value of d_{AB} changes as 6.2 nm, 20.2 nm, 27.3 nm, 28.5 nm, 40.5 nm, 41.8 nm, when going from the P(MBL-*b*-HMA_1-*b*-MBL)$_1$ to P(MBL-*b*-HMA_6-*b*-MBL)$_6$, respectively. In addition to the main SAXS peak, additional higher order of diffractions are detected, suggesting good degree of structural ordering, which is in line with the DSC results. Assignment of the peaks reveals the

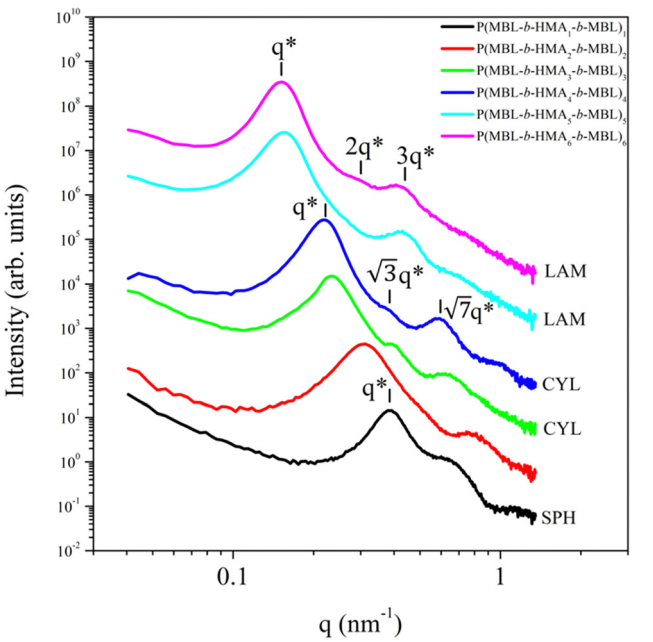

Fig. 2 SAXS curves for the P(MBL-*b*-$PHMA_x$-*b*-PMBL)$_x$ terblock copolymers.

geometry of the BCP morphology, which changes from spherical to cylindrical and then lamellar, in agreement to the change in the relative content of the MBL blocks.[26] Due to the use of a RAFT polymerisation approach, the size polydispersity of the blocks is limited, as witnessed by the clear form factor oscillation detected in the SAXS curve for the P(MBL-*b*-PHMA$_1$-*b*-PMBL)$_1$ sample with spherical morphology. Notably, the SAXS profile for the P(MBL-*b*-PHMA$_5$-*b*-PMBL)$_5$ sample with the lamellar morphology shows clear extinction of the 2q^* peak, as a result of the equal thickness of the domain A and domain B blocks.

3.5. Rheology

All copolymers were subjected to a dynamic frequency sweep at three different temperatures (110, 160 and 200 °C) within the linear viscoelastic regime (Fig. 3). The rheological behaviour was compared between the different weight ratios of the individual polymers. The complex viscosity, obtained from the dynamic frequency sweep tests, was used as the main rheological function for comparison. By varying the ratio between the hard outer and soft inner blocks, one would expect an increase of the complex viscosity with a higher wt% of MBL, which is confirmed within the range of temperatures studied. Secondly, an increase in the temperature shifts the curves downwards to a lower complex viscosity, originating from the middle PHMA block which becomes more flexible and renders the thermoplastic elastomer softer. Last, all copolymers exhibit non-Newtonian behaviour across the temperature range, illustrated by a decrease in apparent viscosity when the strain is increased (*i.e.* shear thinning effect).[27,28]

The results of the frequency sweep of the terblock copolymers are shown (Fig. 3), and a few things can be concluded based on these results. Firstly, an increase of the complex viscosity is evident with an increase of the amount of PMBL incorporated into the structure. Secondly, an increase in temperature leads to a decrease in complex viscosity. This is also expected as the polymer chains of the softer middle block hexyl methacrylate become more flexible because higher temperature means a softening effect for thermoplastic elastomers. All copolymers exhibit non-Newtonian behaviour at all of the temperatures. Only shear thinning behaviour can be seen within the probed frequency range.[27,28] This makes it possible to capture the observed data by plotting a power law function in the form of eqn (2). These fittings can be found in Tables S3–S5 of the ESI.†

$$\eta^* = a\omega^{-n} \quad (2)$$

Here η^* is the complex viscosity, ω is the oscillation frequency, a is the flow consistency, and n is the shear thinning slope. This empirical equation can eventually be used to predict the complex viscosity at any higher frequency or processing rate, typical for extrusion or injection moulding. For the 110 and 160 °C fitting there is no significant change in the shear thinning. This can be explained by the fact that the PMBL segments are not above its apparent T_g. When the experimental temperatures reach 200 °C a change in the shear thinning is observed. Now, the whole terblock copolymer is in the rubbery phase resulting in a decrease of complex viscosity. It is noteworthy that the decrease of the shear thinning slope is more noticeable for P(MBL-*b*-HMA$_6$-*b*-MBL)$_6$ compared to P(MBL-*b*-HMA$_1$-*b*-MBL)$_1$. This is the result of the length of the PMBL segment of P(MBL-*b*-HMA$_6$-*b*-MBL)$_6$. The majority of P(MBL-*b*-HMA$_1$-*b*-MBL)$_1$ chain is already in its rubbery state leading to less noticeable effect of decrease in the shear thinning slope. The flow consistency a is increasing with the length the PMBL segment due to the increase of the PMBL molar/weight fraction. At all three temperatures an increase of flow consistency is observed with an increasing amount of PMBL ratio. Furthermore, a decrease is observed at higher temperatures. With eqn (2) it is possible to predict the apparent viscosity of the copolymers at higher frequencies or processing rates, typical for extrusion (500–1000 rad s^{-1}) or injection moulding (10 000 rad s^{-1}), given in Tables S6–S8 (ESI†).[29] It also allows for the comparison of these predictions to that of SBS(-blends) from previous work.[12] P(MBL-*b*-HMA$_1$-*b*-MBL)$_1$ to P(MBL-*b*-HMA$_5$-*b*-MBL)$_5$ have comparable viscosities rendering the block copolymer not much more difficult for processability. However, P(MBL-*b*-HMA$_6$-*b*-MBL)$_6$ is extremely stiff which could be a

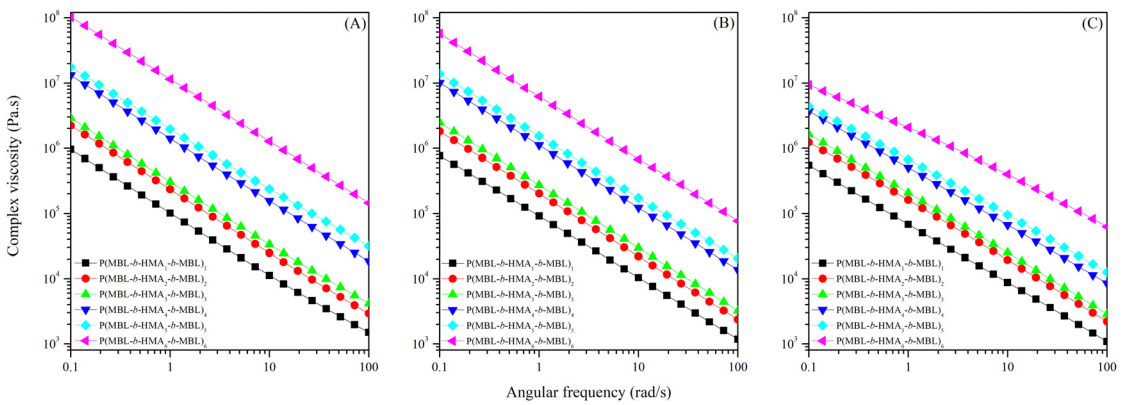

Fig. 3 Frequency sweep of the P(MBL-*b*-PHMA$_x$-*b*-PMBL)$_x$ terblock copolymers at different temperatures (A) 110 °C, (B) 160 °C, (C) 200 °C.

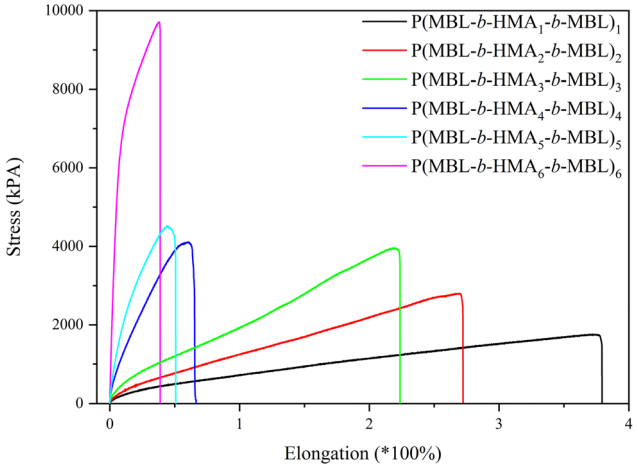

Fig. 4 Stress–strain curve of the P(MBL-*b*-PHMA$_x$-*b*-PMBL)$_x$ terblock copolymers.

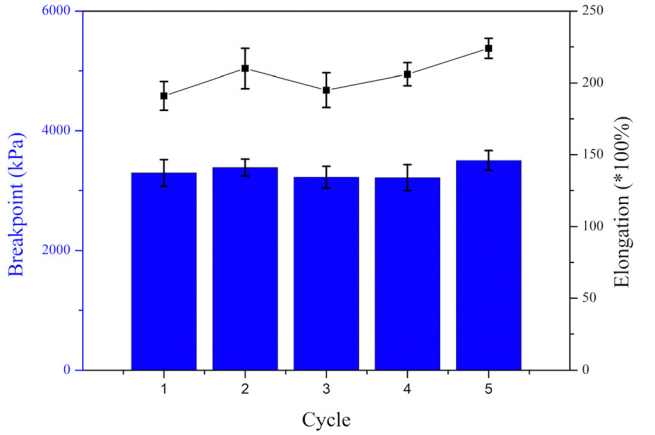

Fig. 5 Tensile strength and elongation at break of P(MBL-*b*-HMA$_3$-*b*-MBL)$_3$ for five cycles with remoulding at 205 °C.

problem for processing due to the high storage modulus from the PMBL segment. This makes the processability of this particular elastomer challenging.

3.6. Tensile test

To further analyse the mechanical properties of the thermoplastic elastomers, stress–strain measurements were conducted on dog bone-shaped samples (Fig. 4). The length of the hard PMBL segments within the linear BAB terblock copolymer plays a crucial part in the mechanical properties of the polymer and may dictate both elongation and yield strength at break. The first sample, P(MBL-*b*-HMA$_1$-*b*-MBL)$_1$ exhibits high elongation at break (375%) but low yield strength at break (1750 kPa), characteristic of rubbery materials. This originates from the short rigid blocks and a long flexible middle segment of that sample. In the opposite scenario (*i.e.* long PMBL segments and short PHMA moiety), such as P(MBL-*b*-HMA$_6$-*b*-MBL)$_6$, short elongation at break (38%) but high yield strength at break (9500 kPa) was observed, typical of a hard rubber. As expected for the whole series, the elongation at break decreases while the yield strength at break increases for samples featuring a higher PMBL ratio. However, note that none of the presently produced elastomers did provide tensile strength and elongation at break close to that of commercial styrene–butadiene–styrene elastomers (SBS) (3500 kPa and 800–1000%, respectively).[12] The maximal elongation for the present terblock copolymers was only about 350%, which can be attributed to the limited segmental mobility of the PMBL blocks, originating from the dipole–dipole interactions and the rigid lactone rings directly attached to the polymer backbone.[30] A similar observation was made by Mosnáček *et al.* for PMBL-based thermoplastic elastomers.[31] Nonetheless, the present straightforward two-step synthesis protocol permits the production of rubbers with tailored and predictable mechanical behaviour.

In previous studies it was established that blending and moulding of SBS elastomers above 200 °C resulted in the formation of crosslinks, due to the large proportion of dangling unsaturated bonds. While beneficial to improve their mechanical properties at high temperature, this also largely impedes their recycling.[12] As evidenced above, the present PMBL-based elastomers have a high thermal stability, which is expected to permit their processing into various shapes, while maintaining chemical integrity due to the absence of unsaturation. To assess this, P(MBL-*b*-HMA$_3$-*b*-MBL)$_3$ was subjected to 5 cycles of tensile testing following by remoulding at 205 °C (Fig. 5) and subsequently measuring both its tensile strength and elongation at break. No significant loss of either parameter is observed after 5 cycles, despite a non-inert atmosphere during the remoulding process. This is in accordance with the decomposition and combustion temperatures of the material (240 °C, Fig. S12, ESI†). This not only makes P(MBL-*b*-HMA-*b*-MBL) elastomers suitable for high temperature applications, but also easily recyclable without loss of mechanical properties.

4. Conclusion

Herein, we demonstrated the facile production of PMBL-based thermoplastic elastomers featuring high thermal stability, tuneable strength and elongation as well as recyclable properties. The P(MBL-*b*-HMA-*b*-MBL) terblock copolymers were produced at 22 g scale in a straightforward two-step synthesis using a bis-functional RAFT agent. This not only permits control of the chain lengths and dispersity, but also ensures the growth of both MBL blocks simultaneously. Varying the amount of monomer for the second polymerisation step enables a tailoring of the soft/hard block ratios and this directly influences the mechanical properties of the resulting elastomers. Additionally, the terblock copolymers can also be heated up to 250 °C without degradation or unwanted crosslinking. While two distinct glass transition temperatures, indicating phase separation of the blocks, excellent viscoelastic properties were observed up to temperatures of ~200 °C, which greatly facilitates their moulding. Furthermore, their mechanical properties are preserved through several cycles of remoulding,

making these P(MBL-*b*-HMA-*b*-MBL) recyclable copolymers excellent candidates for high temperature applications.

Author contributions

Friso G. Versteeg: conceptualization, data curation, formal analysis, investigation, methodology, validation, visualization, writing – original draft. Théophile Pelras: conceptualization, data curation, formal analysis, investigation, methodology, validation, visualization, writing – original draft. Giuseppe Portale: investigation, validation, writing – original draft. Francesco Picchioni: funding acquisition, project administration, supervision, validation, writing – review & editing.

Data availability

The authors confirm that the data supporting the findings of this study are available within the article [and/or] its ESI.† All characterization techniques are thoroughly discussed in the main article and ESI.†

Conflicts of interest

There are no conflicts to declare.

Acknowledgements

The authors want to express their gratitude to Prof. Dr Loos for providing the funding of Dr Pelras. Furthermore, the authors would like to thank Dr Parisi for his valuable input on the rheology results. This work was financially supported by SNN (Northern Netherlands Alliance) and the Province of Groningen *via* an EFRO (European Fonds for Regional Development) sFubsidies program. This research received funding from the Dutch Research Council (NWO) in the framework of the ENW PPP Fund for the top sectors and from the Ministry of Economic Affairs in the framework of the 'PPS-Toeslagregeling'.

References

1 R. J. Spontak and N. P. Patel, Thermoplastic Elastomers: Fundamentals and Applications, *Curr. Opin. Colloid Interface Sci.*, 2000, **5**(5–6), 333–340, DOI: **10.1016/S1359-0294(00)00070-4**.

2 G. D. Airey, Rheological Properties of Styrene Butadiene Styrene Polymer Modified Road Bitumens, *Fuel*, 2003, **82**(14), 1709–1719, DOI: **10.1016/S0016-2361(03)00146-7**.

3 F. G. Versteeg, G. D. M. R. Lima, F. Picchioni and P. Druetta, Solubility of Supercritical CO_2 in Polystyrene, *J. Supercrit. Fluids*, 2024, 106374, DOI: **10.1016/J.SUPFLU.2024.106374**.

4 D. Juárez, S. Ferrand, O. Fenollar, V. Fombuena and R. Balart, Improvement of Thermal Inertia of Styrene-Ethylene/Butylene-Styrene (SEBS) Polymers by Addition of Microencapsulated Phase Change Materials (PCMs), *Eur. Polym. J.*, 2011, **47**(2), 153–161, DOI: **10.1016/J.EURPOLYMJ.2010.11.004**.

5 H. Feng, Z. Feng and L. Shen, Miscibility, Microstructure, and Dynamics of Blends Containing Block Copolymer. 2. Microstructure of Blends of Homopolystyrene with Styrene-Butadiene Block Copolymers, *Macromolecules*, 1994, **27**, 7835–7839.

6 G. G. Ferrer, M. Salmerón Sánchez, E. Verdú Sánchez, F. R. Colomer and J. G. Ribelles, Blends of Styrene–Butadiene–Styrene Triblock Copolymer and Isotactic Polypropylene: Morphology and Thermomechanical Properties, *Polym. Int.*, 2000, **49**, 853–859, DOI: **10.1002/1097-0126**.

7 F. Picchioni, E. Casentini, E. Passaglia and G. Ruggeri, Blends of SBS Triblock Copolymer with Poly(2,6-Dimethyl-1,4-Phenylene Oxide)/Polystyrene Mixture, *J. Appl. Polym. Sci.*, 2003, **88**(11), 2698–2705, DOI: **10.1002/APP.12117**.

8 F. G. Versteeg, N. C. Hegeman, K. O. Sebakhy and F. Picchioni, RAFT Polymerization of a Biorenewable/Sustainable Monomer via a Green Process, *Macromol. Rapid Commun.*, 2022, **43**(13), 2200045, DOI: **10.1002/MARC.202200045**.

9 J. T. Trotta, M. Jin, K. J. Stawiasz, Q. Michaudel, W. L. Chen and B. P. Fors, Synthesis of Methylene Butyrolactone Polymers from Itaconic Acid, *J. Polym. Sci., Part A: Polym. Chem.*, 2017, **55**(17), 2730–2737, DOI: **10.1002/POLA.28654**.

10 J. Mosnáček and K. Matyjaszewski, Atom Transfer Radical Polymerization of Tulipalin A: A Naturally Renewable Monomer, *Macromolecules*, 2008, **41**(15), 5509–5511, DOI: **10.1021/MA8010813/SUPPL_FILE/MA8010813-FILE003.PDF**.

11 V. Graur, A. Mukherjee, K. O. Sebakhy and R. K. Bose, Initiated Chemical Vapor Deposition (ICVD) of Bio-Based Poly(Tulipalin A) Coatings: Structure and Material Properties, *Polymers*, 2022, **14**(19), 3993, DOI: **10.3390/POLYM14193993**.

12 F. G. Versteeg, A. Raharjanto, D. Parisi and F. Picchioni, A Novel SBS Compound via Blending with PS-*b*-PMBL Diblock Copolymer for Enhanced Mechanical Properties, *Rubber Chem. Technol.*, 2024, **97**(2), 162–189, DOI: **10.5254/RCT-D-23-00037**.

13 B. Wang, Y. Wang, S. Du, J. Zhu and S. Ma, Upcycling of Thermosetting Polymers into High-Value Materials, *Mater. Horiz.*, 2023, **10**(1), 41–51, DOI: **10.1039/D2MH01128J**.

14 E. F. J. Rettler, T. Rudolph, A. Hanisch, S. Hoeppener, M. Retsch, U. S. Schubert and F. H. Schacher, UV-Induced Crosslinking of the Polybutadiene Domains in Lamellar Polystyrene-Block-Polybutadiene Block Copolymer Films – An in-Depth Study, *Polymer*, 2012, **53**(25), 5641–5648, DOI: **10.1016/J.POLYMER.2012.09.054**.

15 K. McCreedy and H. Keskkula, Effect of Thermal Crosslinking on Decomposition of Polybutadiene, *Polymer*, 1979, **20**(9), 1155–1159, DOI: **10.1016/0032-3861(79)90309-4**.

16 A. Juhari, J. Mosnáček, J. A. Yoon, A. Nese, K. Koynov, T. Kowalewski and K. Matyjaszewski, Star-like Poly(*n*-Butyl Acrylate)-*b*-Poly(α-Methylene-γ-Butyrolactone) Block Copolymers for High Temperature Thermoplastic Elastomers Applications, *Polymer*, 2010, **51**(21), 4806–4813, DOI: **10.1016/J.POLYMER.2010.08.017**.

17 L. Frazer, Radical Departure: Polymerization Does More With Less, *Environ. Health Perspect.*, 2007, **115**(5), A258, DOI: 10.1289/EHP.115-A258.

18 Q. Hu, S. Gan, Y. Bao, Y. Zhang, D. Han and L. Niu, Controlled/"Living" Radical Polymerization-Based Signal Amplification Strategies for Biosensing, *J. Mater. Chem. B*, 2020, **8**(16), 3327–3340, DOI: 10.1039/C9TB02419K.

19 S. Perrier, 50th Anniversary Perspective: RAFT Polymerization – A User Guide, *Macromolecules*, 2017, **50**(19), 7433–7447, DOI: 10.1021/ACS.MACROMOL.7B00767/ASSET/IMAGES/LARGE/MA-2017-00767N_0008.JPEG.

20 W. Fu and B. Zhao, Thermoreversible Physically Cross-linked Hydrogels from UCST-Type Thermosensitive ABA Linear Triblock Copolymers, *Polym. Chem.*, 2016, **7**(45), 6980–6991, DOI: 10.1039/C6PY01517D.

21 K. Satoh, D. H. Lee, K. Nagai and M. Kamigaito, Precision Synthesis of Bio-Based Acrylic Thermoplastic Elastomer by RAFT Polymerization of Itaconic Acid Derivatives, *Macromol. Rapid Commun.*, 2014, **35**(2), 161–167, DOI: 10.1002/MARC.201300638.

22 S. S. Rogers and L. Mandelkern, Glass Formation in Polymers. I. The Glass Transitions of the Poly-(n-Alkyl Methacrylates), *J. Phys. Chem.*, 1957, **61**(7), 985–990, DOI: 10.1021/J150553A033.

23 A. Elshewy, M. El Hariri El Nokab, J. Es Sayed, Y. A. Alassmy, M. M. Abduljawad, D. R. D'hooge, P. H. M. Van Steenberge, M. H. Habib and K. O. Sebakhy, Surfactant-Free Peroxidase-Mediated Enzymatic Polymerization of a Biorenewable Butyrolactone Monomer *via* a Green Approach: Synthesis of Sustainable Biobased Latexes, *ACS Appl. Polym. Mater.*, 2024, **6**(1), 115–125, DOI: 10.1021/ACSAPM.3C01740/ASSET/IMAGES/LARGE/AP3C01740_0007.JPEG.

24 T. Pelras, A. H. Hofman, L. M. H. Germain, A. M. C. Maan, K. Loos and M. Kamperman, Strong Anionic/Charge-Neutral Block Copolymers from Cu(0)-Mediated Reversible Deactivation Radical Polymerization, *Macromolecules*, 2022, **55**(19), 8795–8807, DOI: 10.1021/ACS.MACROMOL.2C01487.

25 T. Pelras, A. Eisenga, G. Érsek, A. Altomare, G. Portale, M. Kamperman and K. Loos, One-Pot Synthesis of Strong Anionic/Charge-Neutral Amphiphilic Block Copolymers, *ACS Macro Lett.*, 2023, **12**(8), 1071–1078, DOI: 10.1021/ACSMACROLETT.3C00355.

26 A. K. Khandpurj, S. Farster, F. S. Bates, I. W. Hamley, A. J. Ryan, W. Brass, K. Almdal and K. Mortensen, Polyisoprene-Polystyrene Diblock Copolymer Phase Diagram near the Order-Disorder Transition, *Macromolecules*, 1995, **28**, 8796–8806.

27 M. A. Rao, *Rheology of Fluid, Semisolid, and Solid Foods*, Springer, NY, 2007, vol. 2, p. 482, DOI: 10.1007/978-0-387-70930-7.

28 L. L. Schramm, *Emulsions, Foams, and Suspensions: Fundamentals and Applications*, Wiley InterScience (Online Service), 2005, p. 448.

29 T. A. Osswald and N. Rudolph, *Polymer Rheology: Fundamentals and Applications*, Hanser, Munich, Germany, 2015.

30 D. C. Green, K. W. Allen, M. L. Kaplan, R. C. Haddon, F. Wudl, E. D. Feit, U. Pittman, W. J. Patterson, S. P. McManus and M. K. Akkapeddi, Poly(α-Methylene-γ-Butyrolactone) Synthesis, Configurational Structure, and Properties, *Macromolecules*, 1979, **12**(4), 546–551, DOI: 10.1021/MA60070A002.

31 J. Mosnáček, J. A. Yoon, A. Juhari, K. Koynov and K. Matyjaszewski, Synthesis, Morphology and Mechanical Properties of Linear Triblock Copolymers Based on Poly(α-Methylene-γ-Butyrolactone), *Polymer*, 2009, **50**(9), 2087–2094, DOI: 10.1016/J.POLYMER.2009.02.037.